Lifetime predictions of exposed geotextiles and geomembranes

R. M. Koerner[1], Y. G. Hsuan[2] and G. R. Koerner[3]

[1]Director Emeritus, Geosynthetic Institute, Folsom, PA, USA,
E-mail: robert.koerner@coe.drexel.edu (corresponding author)
[2]Professor, Drexel University, Philadelphia, PA, USA, E-mail: ghsuan@coe.drexel.edu
[3]Director, Geosynthetic Institute, Folsom, PA, USA, E-mail: gsigeokoerner@gmail.com

Received 20 April 2016, revised 11 August 2016, accepted 12 August 2016

ABSTRACT: A very frequently asked question regarding all types of geosynthetics is, 'How long will they last?' This paper answers the question for exposed geotextiles and geomembranes, assuming that they were properly designed and installed. Furthermore, it compares these new results to the earlier lifetime prediction results of a covered geomembrane. Nonexposed (or covered) lifetime conditions for a 1.5 mm thick high-density polyethylene (HDPE) geomembrane have previously been evaluated and published. Landfill incubation devices at four elevated temperatures of 85, 75, 65 and 55°C were used in the prediction in order to reach 50% of retained strength and elongation. Considering the three stages of (i) depletion of antioxidants, (ii) induction time, and (iii) 50% reduction in mechanical properties, the lifetime extrapolation was made down to 20°C. The 50% reduction value (called halflife throughout the paper) for this geomembrane under these conditions was approximately 450 years. Since the laboratory incubation times took 12 years, other nonexposed geosynthetics were not evaluated under the supposition that the covered situation is generally a moot point for most geosynthetics in their customary applications. For exposed (or uncovered) geosynthetics, however, the situation is quite different. Ultraviolet radiation, elevated temperature and full oxygen are available, which shortens the service lifetime, but how much? For evaluation of this situation, the authors utilized laboratory ultraviolet fluorescent tube weathering devices, as per ASTM D7238, for incubation purposes. Seven different geotextiles and five different geomembranes were evaluated. Each material was incubated at 80, 70 and 60°C until a 50% reduction of strength and elongation occurred. The data was then extrapolated down to 20°C for laboratory halflife values and for comparison with the nonexposed condition. The ratio of nonexposed to exposed lifetime for HDPE geomembranes is approximately seven. The calculations for the 12 exposed geosynthetics then progressed to using site-specific radiation to obtain an equivalent field halflife. Phoenix, Arizona, conditions are illustrated although the procedure is applicable worldwide. Halflife predictions for the geotextiles vary from a few months for the needle punched nonwovens to up to 10 years for monofilaments and high antioxidant formulated products. Results for geomembranes vary from 47 to 97 years, with HDPE being the highest. These exposed halflife results (which took 12 years of laboratory incubation to achieve) are felt to be most interesting and are presented for the first time to an international audience.

KEYWORDS: Geosynthetics, Accelerated incubations, Geomembrane, Geotextile, Laboratory simulation, Lifetime prediction, Long-term degradation

REFERENCE: Koerner, R. M., Hsuan, Y. G. and Koerner, G. R. (2016). Lifetime predictions of exposed geotextiles and geomembranes. *Geosynthetics International*. [http://dx.doi.org/10.1680/jgein.16.00026]

1. INTRODUCTION

The Geosynthetic Materials Association (GMA) Techline is a worldwide on-line service that has existed since 2004, answering geosynthetic questions of all types and applications. It is serviced by the technical personnel of the Geosynthetic Institute (Koerner and Koerner 2011). Since its inception, there have been slightly over 3000 questions placed in seven different categories. One of these categories focuses specifically on geosynthetic lifetime. As seen in Figure 1a, there have been a consistent 100 questions asked for each of the 500 reported increments: in total 591 out of 3000, or 19.7% of all questions. These 591 lifetime questions have been further analyzed as shown in Figure 1b. In all, 49% of the questions were on nonexposed (or covered) geosynthetics, 30% on exposed (or uncovered) geosynthetics, and the remainder on chemical or other issues. In response to this ongoing interest, research on

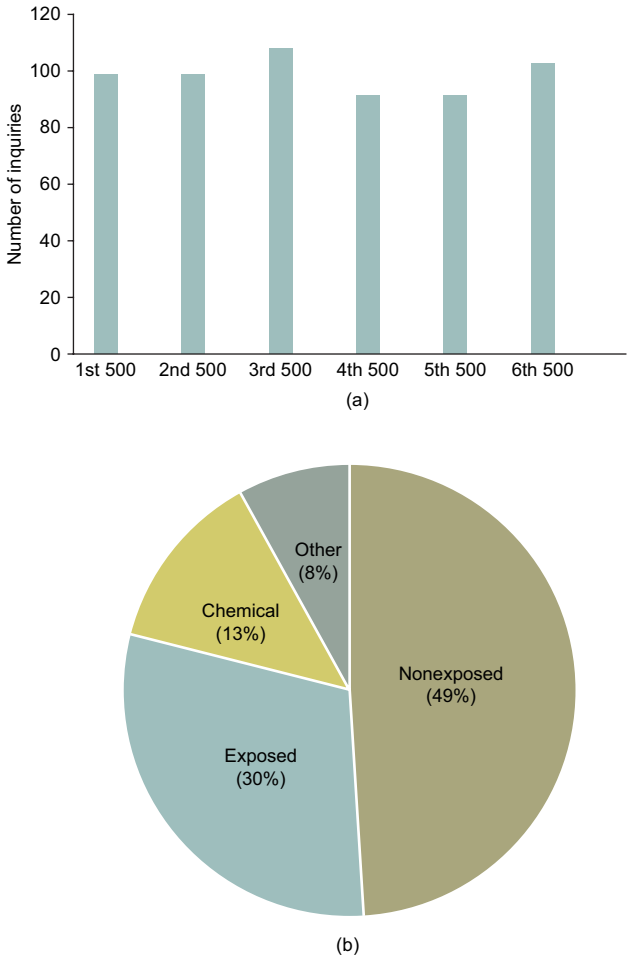

Figure 1. Lifetime questions appearing in the GMA Techline answering service since its inception in 2004. (a) Total questions on lifetime of geosynthetics (b) Lifetime questions by topic

nonexposed lifetime prediction between 1987 and 2000 was undertaken and published, followed by new research on exposed lifetime between 2002 and the present on exposed lifetime predictions. These exposed lifetime results are presented for the first time in this paper.

It is important to note that these lifetime questions and indeed this entire paper do not address many known causes of inadequate geosynthetic performance. For example, the paper does not address

- improper design and/or testing
- blemishes and defects in manufacturing
- improper subgrade preparation
- damage caused during backfilling
- damage caused during maintenance operations
- damage caused during service lifetime (accidents, large animals, etc.)
- tensile and torsional stresses occurring during installation and service lifetime
- stress cracking of crystalline materials, e.g., HDPE geomembranes.

What this paper does address, however, are the long-term degradation mechanisms shown in Table 1. They are counterpointed against the type of resin from which the geosynthetic is manufactured. A brief discussion review of each mechanism follows, but other more complete reviews are also available (e.g., Hsuan *et al*. 2008; Koerner 2012; Greenwood *et al*. 2015; Allen 2016 and others).

Here it is seen that when the geosynthetic is exposed, ultraviolet radiation is a major degradation issue for all geosynthetics but to greatly different degrees. The degradation varies with the resin type and its specific formulation, but also with the specific surface area of the material. As will be shown, geotextiles (particularly needle punched nonwovens) are much more susceptible when exposed than geomembranes.

Oxidation is also a degradation mechanism with exposed geosynthetics; air, being 21% oxygen, is most aggressive. Covered geosynthetics, being exposed to less oxygen, are subject to less aggressive conditions and, if the backfilled geosynthetic is in an anaerobic atmosphere, the issue is not applicable. Thus oxidation is not only resin/formulation specific, it is also site-specific.

Hydrolysis is mainly an issue for polyester geosynthetics, but is only a major consideration if the water has a pH less than 3.0 (called internal hydrolysis) or greater than 10.0 (called external hydrolysis). See Davis (1989) and Elias *et al*. (2001) for details.

Chemicals can be a concern: recall that 13% of the degradation questions in Figure 1b were on this topic, where the most aggressive liquids to geosynthetics are hydrocarbons. Diffusion into the structure of the resin causes swelling and bond breaking to varying degrees. There are charts and tables available, but all are generalized and lack specificity with respect to a particular situation. See van Zanten (1986) for such a chemical resistance chart for a variety of polymer resins. That said, if a situation is of concern, product-specific and

Table 1. Long-term degradation mechanism (Koerner 2012)

Mechanism	Polyethylene (PE)	Polypropylene (PP)	Polyester (PET)	Polyvinyl chloride (PVC)
UV radiation	← Major to all resins but only when exposed →			
Oxidation	← Concern to all resins but to varying degrees →			
Hydrolysis	← No major concern except for PET at high and low pH values →			
Chemical	← Concern over aggressive chemicals, like hydrocarbons, for all resins →			
Radioactive	← Only a concern with respect to high level radioactive waste →			
Biological	← No concern over bacteria or fungi →			
Migration	← No concern except for plasticizers →			
Temperature	← Heat accelerates all of above mechanisms →			

chemical-specific conditions can be replicated in the laboratory or field to evaluate if, and to what degree, they are of concern. Given that, this paper does not address chemical degradation.

Degradation from radioactive waste is generally considered to be a possible concern for high level and transuranic waste disposal and containment. Conversely, for low-level waste and uranium mill tailings, the general opinion is that the activity level is less than that required to create bond breaking and molecular chain scission. See Kane and Widmayer (1989) and Hsuan *et al.* (2008) for additional information. It will not be addressed here.

Biological degradation has often been mentioned as a concern, but it is generally agreed among microbiologists that geosynthetic resins are not sensitive to bacteria and fungi since the molecular weights are too high for attachment and subsequent consumption; see Rios and Gealt (1989). There are laboratory tests available, e.g., Ionescu *et al.* (1982), but they are seldom employed. The above said, animals of various types (rodents, moles, muskrats, deer, moose and bears) have caused damage to both covered and exposed geosynthetics, but they are beyond consideration for the purposes of this paper.

Migration of components in a specific formulation has seen limited investigation, with the exception of the plasticizers associated with PVC. See Kırbaş *et al.* (1999), Liang *et al.* (2008) and Nalli *et al.* (2011) for additional information. Migration of some antioxidants has also been mentioned, but no references appear to be available. That said, migration of components will not be specifically addressed in this paper except in the context of how it modifies the general materials behavior.

Regarding temperature effects on geosynthetics, heat and cold cause a softening and stiffening, respectively, as would be expected. For geosynthetics, high temperatures slightly increase flexibility, and ASTM D1388 can be used to quantify the behavior. The ASTM test method (ASTM D746) addresses the effect of cold temperatures on plastics and, in particular, on brittleness and impact strength. For most geosynthetics, cold ambient temperature is generally not an important degradation topic.

That said, high temperatures do cause all of the above-mentioned polymer degradation mechanisms to occur progressively more rapidly and even at an accelerated rate. In fact, at the heart of elevated temperature incubation and subsequent lifetime prediction techniques using an extrapolation process is the incubation of samples, and periodic testing of laboratory specimens at high temperatures (e.g., 80, 70 and 60°C) and then extrapolation of the resulting degradation trend down to field anticipated temperatures. Thus, high temperature is an acceleration phenomenon acting with other degradation mechanisms such as ultraviolet light (if exposed), oxidation, hydrolysis, chemicals, radiation, biological, migration and so on. As such, elevated laboratory temperature testing will form the critical enabling variable for lifetime prediction of both laboratory and field geosynthetics, which is the focus of the paper.

2. PAST RESULTS FOR NONEXPOSED HDPE GEOMEMBRANES

This section presents the concept of using elevated temperature incubation for long-term degradation and then extrapolation of the test results to lower (presumably site-specific) temperature for lifetime prediction. The section then illustrates the concept for a covered HDPE geomembrane in a simulated landfill liner application.

2.1. Landfill simulation cells for nonexposed geomembrane lifetime study

For any lifetime prediction procedure, the initial consideration for proper laboratory simulation is obviously important. In the example of a nonexposed 1.5 mm thick HDPE geomembrane, the simulation was of a liner situated under 50 m of solid waste, with 300 mm of liquid head above and atmospheric conditions below. The elevated temperature incubations were at 85, 75, 65 and 55°C. Five replicate cells were constructed at each temperature (see Figure 2). Heat tapes were wrapped around the steel cells and insulated accordingly. In the context of the degradation mechanisms listed in Table 1, oxidation, hydrolysis, migration, elevated temperatures

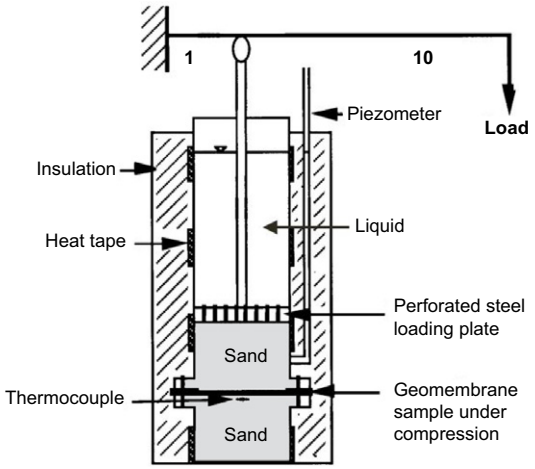

Figure 2. Cross section and actual landfill simulation cells (photograph courtesy of GSI), (a) landfill simulation cell details, (b) 20 landfill simulation cells

and compressive stress were being imposed on the candidate samples.

2.2. Generalized behavior and extrapolation procedure

For the majority of formulations used in geosynthetic applications there are three distinct stages as far as long-term degradation and lifetime prediction are concerned. They are

- stage A: antioxidant depletion time
- stage B: induction time
- stage C: time for loss of strength and/or elongation to a targeted value.

In this third stage, a reduction of strength or elongation to 50% of the material's as-manufactured values is the general target. This is called the halflife, a term used throughout the polymer industry, e.g., gas pipelines, water pipelines, cable shielding applications, suspension bridge cables, and so on. However, it is important to recognize that after halflife is reached there is a time period until end-of-life (EOL) is reached. Thus, halflife is a conservative estimate in lifetime prediction studies. The three stages are shown diagrammatically in Figure 3a as incubation time versus measured property (strength, elongation, etc.) values. Figure 3b illustrates how the halflife values are obtained.

Once the halflives of each temperature are obtained they are plotted on another graph of inverse temperature versus reaction rate, the latter being the inverse of the halflife times. In Figure 4a, the reaction rate is assumed to be semi-logarithmic. However, for physical and/or mechanical reactions the authors feel that it can be arithmetic. The actual data points are connected using a least squares fitting routine (the slope being the 'activation energy') and then extrapolated down to the desired temperature at the field site under consideration. As seen in Figure 4b, 20°C will be used since 20 year field monitoring data is available on a 1.5 mm thick HDPE geomembrane under approximately 50 m of municipal solid waste, see Koerner and Koerner (2014). Once the reaction rate at 20°C is obtained, a ratio with any one of the measured points can be used to calculate the estimated halflife value.

2.3. Estimated halflife of a 1.5 mm thick HDPE geomembrane

Initially financed by a U.S. Environmental Protection Agency grant in 1987 to Drexel's Geosynthetic Research Institute, the fabrication of 20 cells shown in Figure 2 began as described previously. Test specimens were retrieved periodically to quantify the three degradation stages illustrated in Figure 3. Using oxidation induction time measurements via ASTM D3895 and ASTM D5885, the four curves of Figure 5a were generated over the initial 24 months of incubation. These data were plotted as illustrated in Figure 5b and extrapolated to 20°C, resulting in an antioxidant depletion time of 200 years using standard OIT and 215 years using high pressure OIT; an average of 207 years will be used.

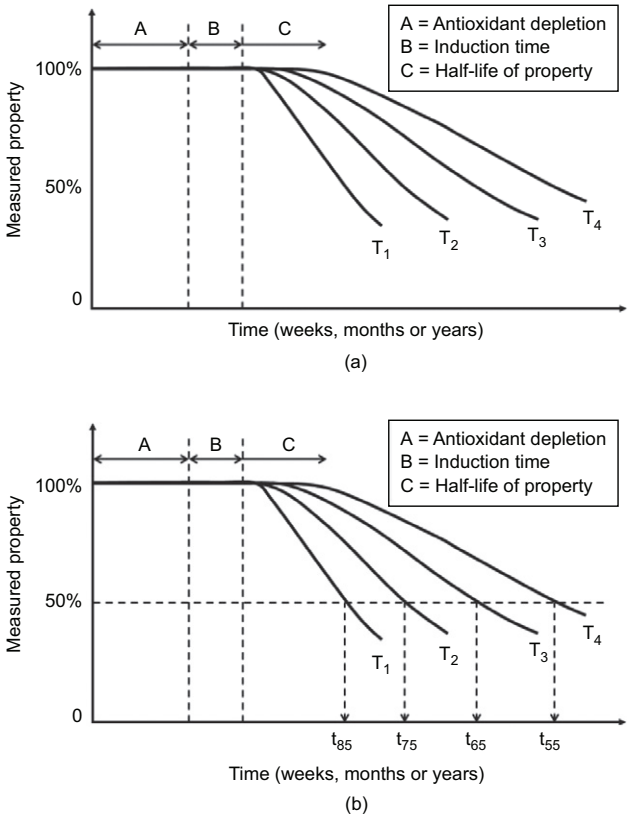

Figure 3. Generalized behavior of property behavior and time for obtaining halflives, (a) incubated property value, (b) halflife determination

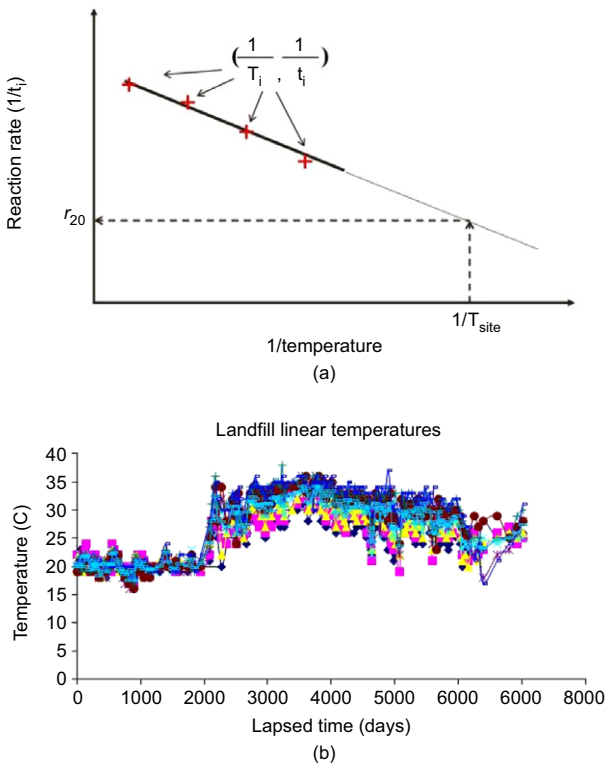

Figure 4. Plotting procedure and extrapolation method to obtain halflife at a specific field temperature, (a) semilog plot for halflife extrapolation, (b) field data of waste backfilled geomembrane to a specific field site condition temperature monitoring over 20 years

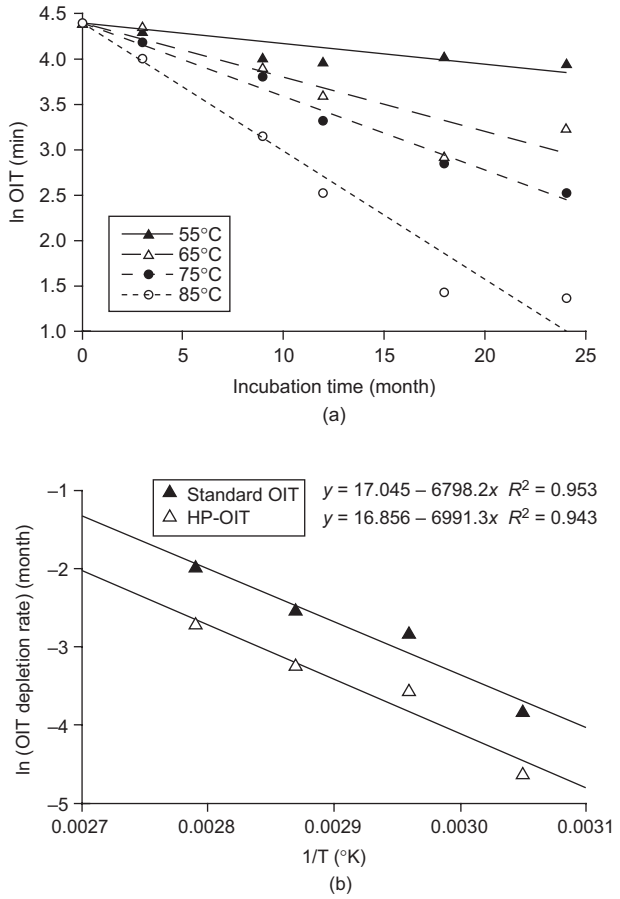

Figure 5. Determination of antioxidant depletion time by two different OIT measurement methods, see Koerner (2012) for details, (a) OIT reduction on a semilog plot, (b) semilog plot of temperature versus OIT reduction

Stage B is the induction time. This is the time from the depletion of antioxidants to the onset of measurable loss of physical or mechanical properties of the test specimens. In order to estimate this stage, the authors located 30 year old HDPE milk and water containers at the bottom of a failed landfill and compared them with similar new containers. As is customary practice, short lifetime milk and water containers do not contain long-term antioxidants, such that there is no stage A as there is for geomembranes. Table 2 shows that yield and modulus values remained the same, but break stress and strain were beginning to decrease beyond the statistical accuracy of the tests. The opinion reached was that the induction time is approximately 30 years at a temperature of 20°C, which was felt to be the situation for these containers.

Insofar as Stage C is concerned, the halflife at each specific incubation temperature is plotted, least squares fitted and extrapolated down to 20°C as previously described. This extrapolation can be done graphically or analytically using the following equation.

$$\frac{r_{\text{T-test}}}{r_{\text{T-site}}} = e^{-E_{\text{act}}/R[1/\text{T-test}-1/\text{T-site}]} \quad (1)$$

where E_{act}/R is the slope of the semilog plot, T-test is the incubated (high) temperature, and T-site is the site-specific (lower) target temperature.

Since the data never reached 50% reductions at the lower incubation temperatures (65 and 55°C) even after 12 years, data from Martin and Gardner (1983) was used for the halflife of tensile strength. The slope of their experimental data, the E_{act}/R value, is −12 800 K. Extrapolation of their 93°C actual incubation temperature (which took 300 h. to complete) to a site-specific temperature of 20°C resulted in the following.

$$\begin{aligned}\frac{r_{93°C}}{r_{20°C}} &= e^{-E_{\text{act}}/R[1/93+273-1/20+273]} \\ &= e^{-12\,800[1/366-1/293]} \\ &= 6083\end{aligned}$$

If the 93°C reaction took 300 h to complete, the comparable 20°C reaction would take

$$\begin{aligned}r_{20°C} &= 6083\ (300) \\ &= 1\ 825\ 000\ \text{h.} \\ &= 208\ \text{yr.}\end{aligned}$$

Thus the predicted time for this particular polymer to reach 50% of its original strength at 20°C is approximately 208 years, which is the authors' predicted halflife for Stage C.

Summarizing the three stages for the predicted lifetime of the covered HDPE geomembrane evaluated leads to an estimated halflife of approximately 450 years at a temperature of 20°C; see Table 3. It is important to recognize, however, that temperatures higher than 20°C will cause lifetime to exponentially decrease. For example, at 30°C (as with wet landfills) the predicted halflife of the same geomembrane would be approximately 166 years. Note, this predicted value of 445 years' halflife while nonexposed will be compared to the same type of

Table 2. Results of tensile testing of new versus old HDPE containers

Property	Milk containers (average of three samples)			Water container (one sample)		
	New (average)	Old (average)	% change	New	Old	% change
Yield stress (MPa)	24	22	n/c[a]	25	24	n/c
Yield strain (%)	11	11	n/c	11	11	n/c
Modulus (MPa)	550	507	n/c	650	580	n/c
Break stress (MPa)	22	14	−36	35	22	−37
Break strain (%)	990	730	−26	1700	970	−43

[a]n/c, no change.

Table 3. Halflife prediction of a nonexposed and covered HDPE geomembrane as a function of in-situ service temperature

In service temperature (°C)	Stage 'A' (years)			Stage B (years)	Stage C (years)	Total prediction[a] (years)
	Standard OIT	High pressure OIT	Average OIT			
20	200	215	207	30	208	445
25	135	144	140	25	100	265
30	95	98	97	20	49	166
35	65	67	66	15	25	106
40	45	47	46	10	13	69

[a]Total = Stage A (average) + Stage B + Stage C.

Table 4. Oldest exhumed geosynthetics showing acceptable performance against various degradation mechanisms

Category	Type	Age in 2014 (yrs.)	Reference
Geomembranes	Non-PE	50	Staff (1984)
Geomembranes	HDPE	35	Haxo (1988)
Geogrids	Uniaxial-PE	35	PGR (1984)
Geotextiles	W-monofilament	50	Barrett (1966)
Geotextiles	NW-needle punched	40	Giroud *et al.* (1977)
Geotextiles	W-slit film	35	Haliburton *et al.* (1980)
Geotextiles	NW-heat bonded	38	Hawkins (2008)

Note: All are apparently ongoing.

geomembrane (1.5 mm thick, black HDPE) in the next section, which is for exposed geosynthetics.

2.4. Commentary on nonexposed geomembrane lifetime

While not in perpetuity, as a few regulations require, a predicted halflife of around 450 years certainly meets almost all applications used in the authors' constructed environment. This project took 12 years to reach the above status, and at a US$450 000 funding level (plus continued maintenance and testing for 12 years) almost precludes the evaluation of other geomembranes in like manner. That said, and due to the semicrystalline nature of HDPE, it is likely that other geomembranes will have shorter halflives but how much so is a matter of pure conjecture. Furthermore, considering different geomembranes, different thicknesses, different formulations, etc., makes a broad-based project of a similar nature simply untenable in the authors' opinion. To further broaden the situation, there are all of the other geosynthetics to consider since by their very nature they are usually nonexposed, that is, they are generally backfilled and covered.

Alternatively, one could also take a 'wait-and-see' approach. In this regard, there is a growing body of case histories by which one can gain confidence in the nonexposed performance of geosynthetics against the mechanisms listed in Table 1. For example, the oldest exhumations of various geosynthetics are given in Table 4. These times are reasonably long, but considering that geosynthetics as a technology began in 1977 (the year of the first organized conference) this is only 39 years to date. Perhaps in a century from now, lifetime predictions of the type presented in this section can begin to be assessed.

3. NEW RESULTS FOR EXPOSED GEOTEXTILES AND GEOMEMBRANES

This section again uses elevated temperature incubation and subsequent testing, followed by extrapolation to lower (presumably site-specific) temperatures for lifetime prediction. It gives halflife times for both laboratory and field, both down to 20°C. This allows comparison with unexposed conditions as well as between laboratory and field results. Phoenix, Arizona, USA, is used for the field conditions, although the procedure is applicable wherever in the world average ultraviolet radiation data is available.

3.1. Ultraviolet degradation and method of incubation

Ultraviolet light is an important cause of degradation for all organic materials, including all of the polymers from which geosynthetics are made. Energy from the sun is divided into three parts

- infrared, with wavelengths longer than 760 nm
- visible, with wavelengths between 760 and 400 nm
- ultraviolet, or UV, with wavelengths shorter 400 nm.

The UV region is further subdivided into UV-A (400 to 315 nm), which causes some polymer damage; UV-B (315 to 280 nm), which causes severe polymer damage; and UV-C (280 to 100 nm), which is only found in outer space, see Figure 6. Furthermore, from summer to winter there are changes in both the intensity and the spectrum of sunlight, the most significant being the loss of shorter wavelengths of UV radiation during the winter months.

Other factors in the UV degradation process of polymers are geographic location, temperature, cloud cover, wind, moisture, atmospheric pollution and product

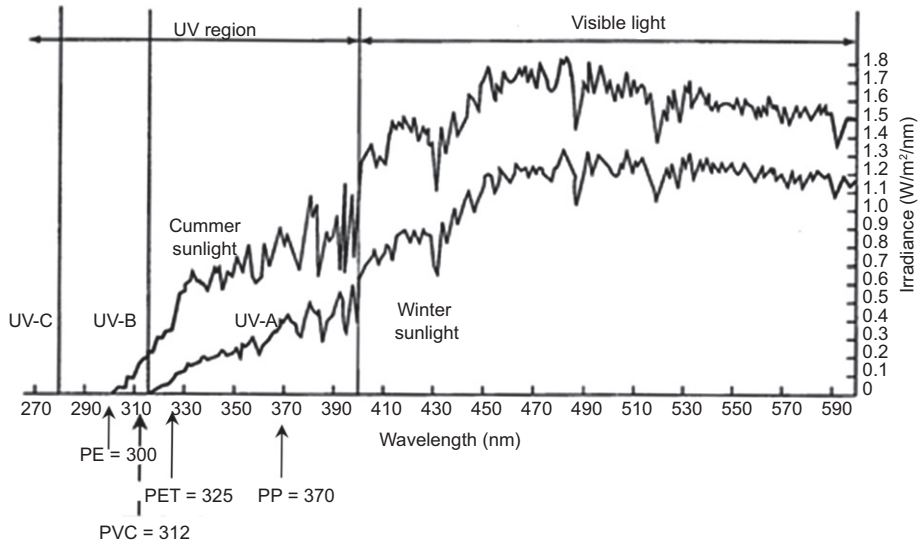

Figure 6. The wavelength spectrum of visible and UV solar radiation (after Q-Panel Co., Cleveland, OH)

orientation. While difficult to assess, these should be considered for field lifetime prediction. Laboratory simulation is critical, however, for it provides the base line degradation under completely controlled conditions such as radiation, temperature, oxidation, and moisture. The critical next step, the extension from laboratory to field predicted lifetimes, is of paramount importance to owners and design engineers for obvious reasons.

For laboratory simulation of sunlight, artificial light sources (tubes or bulbs) are generally compared with worst-case conditions, or the 'solar maximum condition'. The actual degradation is caused by photons of light breaking the polymer's chemical bonds. For each type of bond, there is a threshold wavelength for bond scission, above which the bonds will not break and below which they will. Thus the short wavelengths are critical. van Zanten (1986) shows that polyethylene is most sensitive to UV degradation around 300 nm, polyvinyl chloride around 312 nm, polyester around 325 nm and polypropylene around 370 nm; that said, they are all within the UV-A or UV-B range of the wavelength spectrum. See Figure 6 for these approximate values of the resins from which most geosynthetics are made.

Of the available laboratory weathering devices, the two most common are xenon arc (ASTM D4355) and ultraviolet fluorescent devices (ASTM D7238); see Figure 7. Both produce spectra in the UV-A and UV-B regions quite accurately (where degradation occurs) but the xenon arc continues into visible light while the UV-fluorescent drops off. In the context of the degradation mechanisms shown in Table 1, both devices incorporate UV radiation, oxidation, hydrolysis and high temperature. That said, essentially everything else, particularly the original cost and maintenance costs, favors the UV-fluorescent device in the authors' opinion. Table 5 illustrates these approximate cost differences between the two incubation methods.

When considering that this study represents a 14 year effort to date, the use of UV-fluorescent devices becomes an obvious choice at least in the context of this GSI-financed research project.

Whatever the exposure protocol, representative test samples are incubated and removed at periodic times, cut into tension test specimens, and evaluated for their retained strength and elongation. The results are then compared to the unexposed geosynthetic for percent retained values. When plotted and extrapolated to lower temperatures, lifetime predictions in laboratory weathering devices can be obtained. Using this information, an extension to specific field locations can be generated albeit with some quite serious assumptions. This specific procedure for seven different geotextiles and five different geomembranes will be provided in the research to follow.

3.2. Methodology used and hypothetical example for halflife predictions

The lifetime prediction procedure that will be followed in this paper is accomplished in three stages: (i) incubation of representative samples at multiple elevated temperatures along with periodic tensile testing of retrieved specimens, (ii) extrapolation of the elevated laboratory temperature testing results down to lower temperatures, and (iii) conversion of the laboratory halflife data into site-specific field halflife predicted lifetimes. These three stages are further described as follows, and will be illustrated using hypothetical data. The actual data for the 12 geosynthetics evaluated can be found in the Supplemental Materials for this paper.

Step (i): incubation procedure

- Select a specific geosynthetic material to be investigated.
- Cut the sample into approximately 12 coupons for each incubation temperature to fit into the device holders, each being 250 × 75 mm in size. Filaments, yarns and ribs can be accommodated similarly to sheet materials.

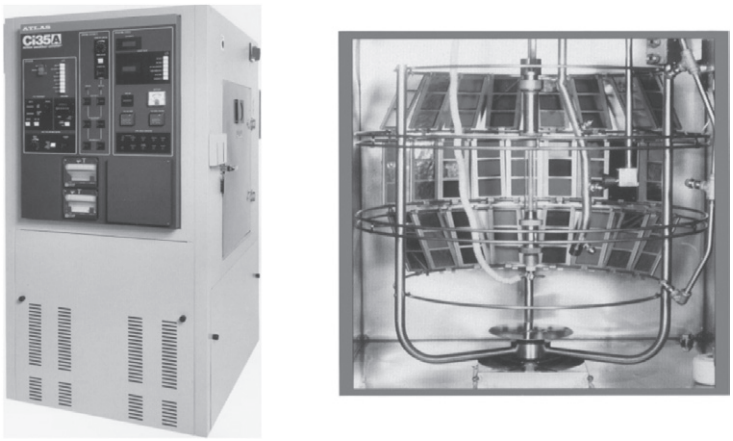

(a)

(b)

Figure 7. Laboratory weathering devices for polymer durability research and development (photographs courtesy of GSI), (a) incubation in xenon arc device as per ASTM D4355, (b) incubation in a UV fluorescent device as per ASTM D7238

Table 5. Relevant costs of commercially available weathering devices

Item/method	(a) Xenon arc	(b) UV-fluorescent
Initial cost	US$70–80 000	US$10–15 000
Tubes/bulbs	US$15 000/year	US$300/year
Power cost	US$5000/year	US$400/year
Water cost	US$3000/year	None
Sewer cost	US$1500/year	None

- Install these coupons in at least three different constant temperature incubation devices.
- Used in this study are three separate devices set at 80°, 70° and 60°C constant temperatures. Each daily cycle is set for 20 hours' lights on and four hours' lights off, the latter with water condensation. The procedure follows ASTM D7238.
- Periodically remove coupons, die cut them into specimens and tensile test them accordingly to established standards. In the cases of individual filaments, yarns or ribs being evaluated, the process is similar.
- Used throughout is a tracking of both tensile strength and elongation at break.
- Compare these gradually decreasing values to original values of non-incubated material for a percent strength and elongation retained and plot the trends as incubation time versus percent retained.

Step (ii): data analysis to reach laboratory lifetimes

- Select 50% retained values for both strength and elongation at each temperature; these are the so-called 'halflives'. Note that the materials are still intact at this point and end-of-life (EOL) is longer. How much so is quite subjective, and beyond the scope of the paper.
- Plot these three temperature data points on a semilogarithmic or arithmetic graph and connect them using a least squares fitting method. The slope of the line is the activation energy. A semilog scale is used in the polymer industry based on the hypothesis that bond breaking by ultraviolet light is a chemical phenomenon as originally suggested by S. Arrhenius in the early 1900s. The authors will do likewise for the laboratory projections.
- Extrapolate the curves down to an arbitrarily selected temperature. A value of 20°C will be used for comparison purposes in all cases.
- This results in the halflife of strength and elongation under these specific laboratory incubation conditions.

Step (iii): data analysis to reach site-specific field lifetimes

- Convert the measured halflife times in the laboratory at the three elevated temperatures to total radiation energy values. This is a known value obtained from the weathering device manufacturer. An example will be given.
- Obtain the ultraviolet radiation at the field location of interest. This is also a known radiation value,

obtained from national or world radiation energy maps.
- Calculate the equivalent time to reach halflife at the field site using the appropriate field radiation.
- Plot these times on an arithmetic graph using a least square fitting method. An arithmetic scale is used since it is felt that field degradation is very likely a composite of physical, chemical and mechanical phenomena. This procedure will be used.
- Extrapolate down to 20°C for halflife predictions based on these 50% loss of strength and elongation data points, assess the results, and make comparisons to the laboratory predicted values, also at 20°C.

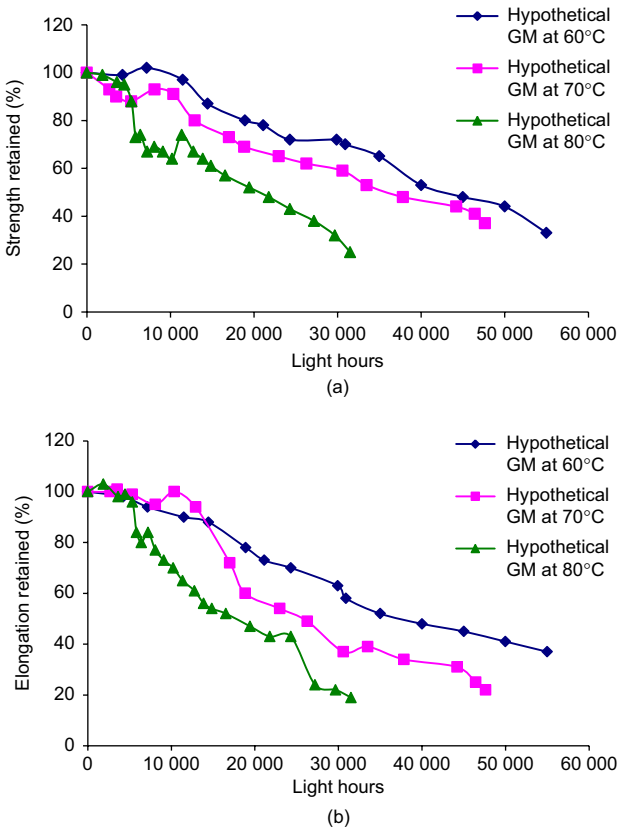

Figure 8. Degradation in strength and elongation behavior of a hypothetical geomembrane at 80°C, 70°C and 60°C incubation in UV fluorescent weathering devices as per ASTM D7238 test method. Note: multiply light hours by 24/20 = 1.2 to obtain total hours

In order to illustrate Step (i) a hypothetical geomembrane is used. Assume that the data of Figure 8 has been generated as just described. Here, the curves of percent retained strength (Figure 8a) and percent retained elongation at break (Figure 8b) are shown to have a gradually decreasing behavior over increasing incubation times in the three weathering devices. Obviously, the lower 60°C temperatures take longer to reach 50% reduction (halflife) than the higher temperature 80°C incubations, with the intermediate 70°C temperature in between. This is the essence of comparative elevated temperature degradation. The 50% reduction values of both strength and elongation are then used in step (ii). In these hypothetical data sets, the curves are generated by connecting the actual measured data points. Experimental variation will be clearly evident. In general, these are single data points and not averages of multiple tests at each time increment. Space in the weathering devices precludes such enhanced accuracy. Also to be noted is that light hours were measured while taking the data, but they were converted by a factor of 24/20 = 1.2 in order to arrive at total hours, which was used in the prediction methods to follow.

As far as step (ii) is concerned, the 50% reductions in strength and elongation, i.e., the halflives, are now plotted on a semilogarithmic graph as shown in Figure 9.

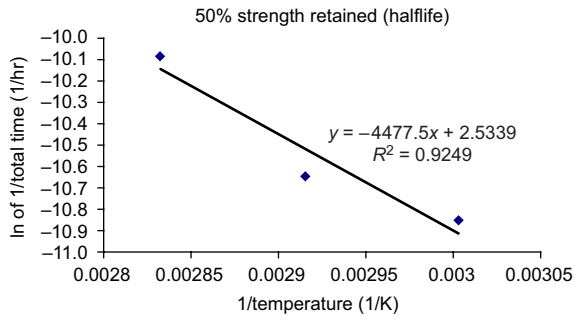

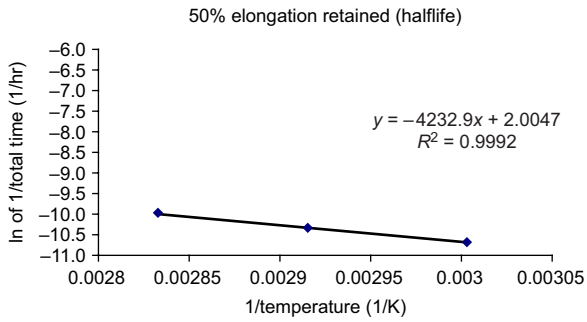

Prediction		
Temperature	Lifetime (hours)	Lifetime (years)
80	24000	2.7
70	42000	4.8
60	51600	5.9
50	83144	9.5
40	129471	14.8
30	207592	23.7
20	343750	39.2

Prediction		
Temperature	Lifetime (hours)	Lifetime (years)
80	21600	2.5
70	31200	3.6
60	44400	5.1
50	66188	7.6
40	100603	11.5
30	157199	17.9
20	253231	28.9

Figure 9. Halflife laboratory predictions of hypothetical geomembrane down to 20°C using fluorescent ultraviolet weathering devices per (ASTM D7238). (Note: Total Hours = 24/20 = 1.2 times light hours)

As mentioned previously, semilog plotting is generally accepted for chemical reactions. Using a least squares fitting routine, the connecting line, which defines the activation energy, can be assessed for the testing accuracy by noting the R^2-values. The closer to unity, the better the fit is to the experimentally generated data. The three point trend lines are then extrapolated in 10 degree increments down to 20°C for assessment and comparative behavior, as shown in the tabulated data. The laboratory predicted halflife of this geomembrane at 20°C is about 39 years for strength and 29 years for elongation.

As far as step (iii) is concerned, the laboratory-generated halflives at each temperature are again used but are now converted from laboratory radiation (which is given by the equipment manufacturer as 42.42 W/m^2 at 340 nm) to site-specific radiation. Phoenix, Arizona, is used in this conversion since it has the highest radiation in the U.S. The reported value (NREL 2012) is 28 MJ/m^2-month. Such data is also available for all regions of the world; see 3 Tier (2011). These converted values for the three incubation temperatures of 80, 70, 60°C are then plotted, connected by a least squares fitting method, and extrapolated in 10 degree increments down to 20°C for the predicted halflife value in the field at the prescribed location. As mentioned previously, an arithmetic plot is used since more than chemical reactions are involved in the field as suggested in Table 1. A sample calculation of the ultraviolet radiation conversion from laboratory to field is as follows:

Example: convert the laboratory-obtained 50% strength retained properties of the data shown in Figure 8, where at 80°C (=20 000 total hours), 70°C (=35 000 total hours) and 60°C (=43 000 total hours) from ultraviolet fluorescent incubation to worst case U. S. field conditions in Phoenix, Arizona, using

- UV-fluorescent (ASTM D7238) irradiance = 42.42 W/m^2 between 250–400 nm wavelengths, which is a property of the weathering device
- UV radiation in Phoenix (hot and dry climate) = 28 MJ/m^2-month, which is available in published literature, as is radiation data on a worldwide basis.

Calculations:

$$\text{Laboratory}\begin{cases} @\ 80°C : 20\,000\ \text{h.} = 72.0 \times 10^6\ \text{s} \times 42.42\ \text{W/m}^2 \div 10^6 \\ \qquad\qquad = 3054\ \text{MJ/m}^2\ \text{total energy} \\ @\ 70°C : 35\,000\ \text{h.} = 126 \times 10^6\ \text{s} \times 42.42\ \text{W/m}^2 \div 10^6 \\ \qquad\qquad = 5345\ \text{MJ/m}^2\ \text{total energy} \\ @\ 60°C : 43\,000\ \text{h.} = 155 \times 10^6\ \text{s} \times 42.42\ \text{W/m}^2 \div 10^6 \\ \qquad\qquad = 6575\ \text{MJ/m}^2\ \text{total energy} \end{cases}$$

$$\text{Field}\begin{cases} @\ 80°C = 3054/28 = 109\ \text{mo.} \times 24/20 = 131\ \text{total months} \\ @\ 70°C = 5345/28 = 191\ \text{mo.} \times 24/20 = 229\ \text{total months} \\ @\ 60°C = 6575/28 = 235\ \text{mo.} \times 24/20 = 282\ \text{total months} \end{cases}$$

Now plot the above data on an arithmetic scale, connect the points using a least squares fitting method, and extrapolate it in 10 degree increments to the average monthly temperature at 20°C for the Phoenix, Arizona, predicted lifetime. Figure 10 illustrates this procedure, where the 50% strength and elongation light hours have been converted to total hours using a 24/20 = 1.2 multiplier and then converted using radiation levels of laboratory to field values as shown in the above example. This ratio is determined, since the UV lights were on for 20 h/day as directed in the test standard. The three temperature values were connected using a least squares fitting routine and then extrapolated in 10°C increments down to 20°C to be comparable to the laboratory extrapolated values of Figure 9. The field predicted halflife in Phoenix, Arizona of this geomembrane at 20°C is 49 years for strength and 41 years for elongation. That said, this is a hypothetical example, but it illustrates the computational procedure. The actual data for the seven geotextiles and five geomembranes evaluated in this study and their results are found in the Supplemental Materials to this paper.

3.3. Halflife prediction values for seven geotextiles

The previous three steps outlined in Section 3.2 have been performed on seven commercially available geotextiles from five different manufacturers. All are black polypropylene products, but the authors do not know the specific formulations. That said, using different formulations, particularly antioxidants, the results will be reflected accordingly. In this regard, direct comparison to the oxidation induction times (OIT) should be made. The various properties are as indicated in Table 6. In Figures 11 through 17 in the supplemental information are the strength and elongation reductions, the laboratory halflife calculations and the field halflife calculations. Commentary on the results and comparisons will be given in Section 3.5 following.

3.4. Halflife prediction values for five geomembranes

The three steps outlined in Section 3.2 have been performed on five commercially available geomembranes from four different manufacturers. The authors do not know the specific formulations, but they all conform to available generic specifications. That said, using different formulations, particularly antioxidants, the result will be reflected accordingly. In this regard, direct comparisons

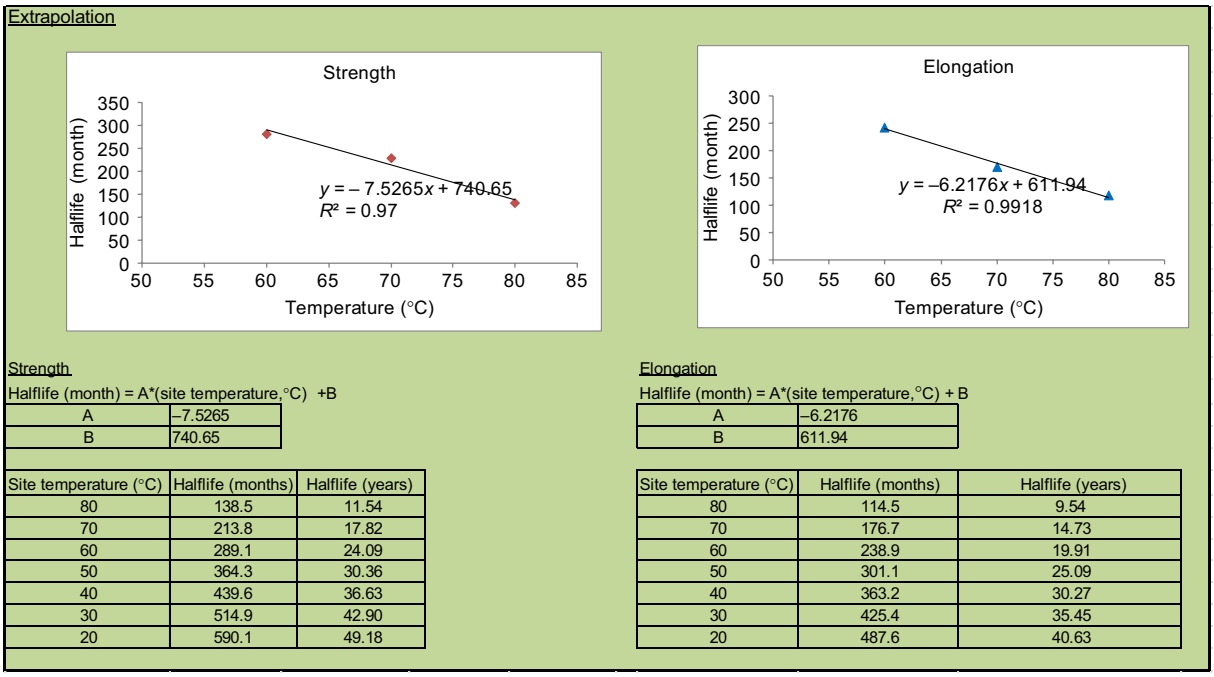

Strength

Halflife (month) = A*(site temperature,°C) +B

A	–7.5265
B	740.65

Site temperature (°C)	Halflife (months)	Halflife (years)
80	138.5	11.54
70	213.8	17.82
60	289.1	24.09
50	364.3	30.36
40	439.6	36.63
30	514.9	42.90
20	590.1	49.18

Elongation

Halflife (month) = A*(site temperature,°C) + B

A	–6.2176
B	611.94

Site temperature (°C)	Halflife (months)	Halflife (years)
80	114.5	9.54
70	176.7	14.73
60	238.9	19.91
50	301.1	25.09
40	363.2	30.27
30	425.4	35.45
20	487.6	40.63

Figure 10. Halflife field predictions in Phoenix, Arizona, of hypothetical geomembrane down to 20°C using fluorescent ultraviolet weathering devices as per ASTM D7238

Table 6. Details of geotextiles evaluated in this study

Structure	Type	Mass (g/m^2)	OIT (min.)	Strength (kN/m)	Elongation (%)	Results[a]
Woven	Monofilament	220	4.7	32.4	18	Figure 11
Woven	Slit film	110	1.8	16.9	13	Figure 12
Nonwoven	Heat bonded	340	14.7	21.4	70	Figure 13
Nonwoven	Needle punched	130	0.9	8.3	51	Figure 14
Nonwoven	Needle punched	180	0	9.5	87	Figure 15
Nonwoven	Needle punched	360	0.19	19.8	115	Figure 16
Nonwoven	Needle punched	480	0.22	28.9	109	Figure 17

[a]These figures are found in the Supplemental Materials for this paper.

Table 7. Details of geomembranes evaluated in this study

Types	Specifications (GRI)	Thickness (mm)	OIT (min.)	Strength (kN/m)	Elongation (%)	Results[a]
HDPE	GM13	1.5	67.0	56.6	750	Figure 18
LLDPE	GM17	1.0	21.1	38.7	760	Figure 19
fPP	GM18	1.0	7.2	14.3	600	Figure 20
EPDM	GM21	1.0	0	10.0	640	Figure 21
PVC (Euro.)	Proprietary	2.5	5.9	47.2	400	Figure 22

[a]These figures are found in the Supplemental Materials for this paper.

to the oxidative induction times (OIT) should be made. The various properties are indicated in Table 7 with selected properties of interest. Figures 18 through 22 are the strength and elongation reductions, the laboratory halflife calculations and the field halflife calculations. They are given in the Supplemental Materials. Discussion on the results and comparisons will be included in Section 3.5 following.

Some commentary about the selected geomembranes is appropriate. With the promulgation of the solid waste landfill regulations by the U.S. Environmental Protection Agency in 1982, geomembranes were required beneath and above the encapsulated solid waste mass. The regulations required the geomembranes to be 0.75 mm thick, except for HDPE, which was required to be 1.50 mm thick. The logic for this doubling of thickness was that HDPE was seamed using extrusion welding. In so doing, the area to be bonded between the overlapping sheets had to be ground using a hand-held grinding wheel. Thus, an unknown amount of material thickness was lost in the

Table 8. Comparative laboratory and field halflives at 20°C for 12 commercially available geosynthetics evaluated in this fourteen-year GSI study

(a) Geotextiles (all PP)	Mass (g/m^2)	Figure no. (supp. data)	Laboratory predicted halflife in years		Phoenix, Arizona, predicted halflife in years	
			Strength	Elongation	Strength	Elongation
Woven, monofilament	220	11	5.7	5.7	10.3	10.3
Woven, slit film	110	12	0.34	0.25	0.76	0.61
Nonwoven, heat bonded	340	13	4.5	4.1	4.9	5.9
Nonwoven, needle punched	130	14	0.22	0.22	0.42	0.55
Nonwoven, needle punched	180	15	0.29	0.21	0.55	0.49
Nonwoven, needle punched	360	16	0.24	0.22	0.58	0.55
Nonwoven, needle punched	480	17	0.28	0.28	0.57	0.60

(b) Geomembranes (various resins)	Thickness (mm)	Figure no. (supp. data)	Laboratory predicted halflife in years		Phoenix, Arizona, predicted halflife in years	
			Strength	Elongation	Strength	Elongation
HDPE	1.5	18	76	69	97	91
LLDPE	1.0	19	49	46	66	63
fPP	1.0	20	50	41	59	54
EPDM	1.0	21	60	70	74	56
PVC (Euro.)	2.5	22	54	54	72	55

process and to compensate for this required a greater thickness to begin with. Conversely, PVC geomembranes were seamed with solvents and EPDM was seamed with a double-sided adhesive tape, thus no material was thinned. Interestingly, neither fPP nor LLDPE were available at the time but they also required grinding and loss of thickness. In this regard, the thicknesses of the geomembranes selected are quite commonly used in myriad applications.

Regarding the HDPE selected, this is 1.5 mm thick, black, and conforms to the GRI-GM13 generic specification. The standard OIT value was 67.0 min and its as-manufactured strength and elongation are given in Table 4 as with the other geomembranes.

Regarding the LLDPE selected, this is 1.0 mm thick since it did not fall under the regulations cited. It is also black and conforms to the GRI-GM17 generic specification. It has an OIT value of 21.1 min.

Regarding the fPP selected, this is a mixture, or blend, of polypropylene and a thermoset rubber and is best made in a reactor rather than blended in an extruder. This particular material was reactor grade. It does not fall under the regulations cited. It is 1.0 mm thick, also black, has a standard OIT value of 7.2 min. and conforms to the GRI-GM18 generic specification.

Regarding the EPDM selected, this is a thermoset polymer, also 1.0 mm thick, black, and conforms to the GRI-GM21 generic specification. It has no antioxidants in the formulation.

Lastly, the PVC that is customarily used in North America follows (ASTM D7176) but it is specifically focused on nonexposed conditions, i.e., for buried applications only. As a result, a European PVC formulation, which has been successfully used for over 40-years in waterproofing dams on a worldwide basis, was selected; see Scuero and Vaschetti (1996) and Cazzuffi (2014). It is 2.5 mm thick, grey, and is only available via the manufacturers' proprietary specification. It has antioxidants with OIT of 5.9 min. and several high molecular weight plasticizers, which are proprietary.

Figures 18 through 22 give the results of the three step process described previously for the five geomembranes listed in Table 7 and are provided in the Supplemental Materials for this paper.

3.5. Comparative results and discussion

The resulting halflife prediction values obtained for the seven geotextiles and the five geomembranes evaluated in this study are presented in Table 8. In each case strength and elongation halflives are given for both laboratory and field results.

In viewing the response curves of Figures 11 through 22 after incubation and the calculated halflives of laboratory and field projections as shown comparatively in Table 8 above, the following is observed regarding the results for the seven geotextiles.

- The strength and elongation retained curves versus incubation times are reasonably well behaved considering that each data point is at a specific incubation time.
- Halflife prediction times for the woven monofilament and nonwoven heat bonded geotextiles are excellent, the former likely due to the low specific surface area of the relatively thick fibers and the latter due to a purposely high antioxidant loading. The latter is also grey in color, while the others are all black.
- The woven slit film and all four needle punched nonwovens resulted in the shortest lifetime predictions.
- Halflife predictions for the four needle punched nonwovens are remarkably similar considering the

differences in mass, i.e., from 130 to 480 g/m^2. This is contrary to the authors' original thinking in their selection, and the results might have been different if there had been a single manufacturer and single formulation.
- For all seven geotextiles the field halflives are greater than the laboratory halflives. Thus, the laboratory incubation is more severe in its degradation than in Phoenix, Arizona.

The following is observed regarding the results of the five geomembranes.

- The strength and elongation retained curves versus incubation times are reasonably well behaved considering each data point is at a specific incubation time. Also, some of the 60°C data is not yet at 50% retained, and thus required estimation. These incubations are ongoing.
- The HDPE results in the longest halflife values in both the laboratory and field situations. That said, its thickness is slightly greater than the others, except for the PVC (European).
- The other four geomembranes have somewhat similar halflife values. That said, there are reverses of strength halflives and elongation halflives within the various geomembranes.
- In general, the field halflives are usually greater than laboratory halflives, but not by as much as was seen for the geotextiles.
- As expected, the differences in halflives between all geotextiles and all geomembranes is huge. Data (not shown) show that geogrids and turf reinforcement yarns are between these extremes, but the paper length precludes presenting this information.

4. CONCLUSIONS

The anticipated service lifetime due to general material degradation of all geosynthetics is invariably asked by owners, regulators and designers, as well as the suppliers, manufacturers and installers that are involved. Other than intentional or accidental damage, the usual degradation mechanisms are (recall Table 1)

- ultraviolet radiation
- oxidation
- hydrolysis
- chemical
- radioactive
- biological
- migration
- temperature.

After an overview of the scope of the paper, each of the above mechanisms was individually described. Of course, each mechanism only has relevance depending on site-specific conditions as well as the specific type of geosynthetic resin and formulation from which it was made. If indeed a specific mechanism is involved, testing organizations have appropriate standards for such laboratory evaluation. These standards were cited accordingly. The results of such testing, however, are usually of a 'go-no go' nature insofar as a final decision is concerned, i.e., they are not meant to be lifetime prediction methods.

Alternatively to testing for a specific mechanism, one can implement field trials to determine lifetime. However, geosynthetics have shown themselves to be so robust when covered as to make this approach impractical; recall Table 4. For example, geotextiles (the most sensitive to long-term degradation of the different geosynthetics) in covered applications have been exhumed with properties approaching their original values after decades of service. This feature of long-term geosynthetic performance when covered shifts the emphasis to behavior when the material is exposed. Exposed geotextile lifetimes are known to be quite short (weeks to a few months) in both hot dry and hot humid climates, while exposed geomembrane performance results in lifetimes of several decades, with the other geosynthetics between the two. To be sure, the type of geosynthetic and its specific formulation is of critical importance and some specially formulated types have been known to last far longer than the typical formulations. The difference between the very long lifetimes when covered versus the much shorter times when exposed are due to three main degradation mechanisms; ultraviolet radiation, high temperatures and full atmospheric oxidation.

These three items lend themselves to commercially available laboratory incubation devices and subsequent testing to predict exposed geosynthetic lifetimes. This is the approach illustrated in the rather lengthy Subsection 3.3 of this paper. Two important situations were illustrated: the extrapolated exposed lifetime at a specific temperature in the laboratory simulation device and the predicted exposed lifetime at a specific field location.

The approach to both laboratory and field predictions is to incubate samples of the candidate geosynthetic in weathering devices set at elevated constant temperatures. Temperatures of 80, 70 and 60°C are used in this study. The weathering devices followed the ASTM D7238 protocol and are known as ultraviolet fluorescent devices. Periodic removal of samples and subsequent test specimens was undertaken, and these were evaluated for their tensile properties of strength and elongation at break. When compared to the original strength and elongation values, a percent retained is calculated. Over the extended incubation time, these percent retained values are plotted until 50% retained is reached. This is known as a 'halflife'. Using the halflife values for each incubation temperature, two different extrapolation approaches down to an arbitrarily selected temperature of 20°C were made. For laboratory lifetimes, a semi-logarithmic graph was used for the process. This is the Arrhenius model for chemical reactions, and is the usual approach for laboratory predictions. For field lifetimes, a radiation conversion of laboratory-to-field was made based on radiation differences, and an arithmetic graphing was used for the

extrapolation process. This assumes that chemical, physical and mechanical processes are involved. Phoenix, Arizona, was used as the field site. The results of these two approaches to the exposed lifetime prediction of seven commercially available geotextiles and five commercially available geomembranes were presented in Figures 11 through 22 found in the Supplemental Materials for this paper. These figures are the major 'bottom line' of the entire 12 year study. The results indicate the following points.

- Lifetime predictions in both laboratory and field are shortest for geotextiles (usually less than one year) and the longest for geomembranes (many decades).
- Laboratory lifetime predictions were shorter than in Phoenix, Arizona, for all geosynthetics evaluated. A shorter time indicates that a more harsh degradation situation occurs in the laboratory than in the field.
- The major reason for the above behavior (rather than being a constant ratio of radiation energies throughout) is that the laboratory extrapolations were semilogarithmic and the field extrapolations were arithmetic. These choices were explained in the text of the paper.
- In all cases, the laboratory and field predictions are impressive and should give users of the respective geosynthetics a good degree of confidence insofar as having quantitative data versus heretofore only qualitative statements about longevity.
- It should also be noted that this entire study focused on the halflife of the respective geosynthetics. End-of-life (EOL) is certainly beyond this, but by how much is extremely site-specific and material specific. At EOL the material will generally degrade in its thickness and fail by 'powdering' or 'cracking' due to some (perhaps even nominal) type of applied stress.

It must be cautioned, however, that the results of this 14 year long study on laboratory incubation and subsequent strength and elongation testing is based on the specific type of geosynthetic, i.e., the polymer and its formulation, of the products evaluated. In general, the authors did not know the formulation specifics (antioxidants, additives and/or fillers). Conclusions must be tempered and utilized accordingly, along with the assumptions stated and the specific products evaluated.

Furthermore, the extension from laboratory predicted lifetimes (semilog scale) to field predicted lifetimes (arithmetic scale) is based solely on ultraviolet radiation differences. Other field-specific conditions, e.g., orientation, moisture, environment, etc., will likely vary the results in some undetermined manner, at least in the context of the results of this study. It should also be mentioned that several incubations at the lower laboratory temperature (60°C) are still ongoing for the geomembranes, and some change in predicted values will likely occur in the future.

That said, lifetime predictions in the hot and dry climate of Phoenix, Arizona, are impressive and are somewhat longer than originally envisioned by the authors. Use of the information, however, must be tempered with the assumptions stated and the specific products evaluated.

In conclusion, it is felt that this type of lifetime prediction for exposed geosynthetics is reasonably simulated in laboratory weathering devices. While such laboratory lifetimes are of value in comparing different products or different formulations of the same product, the process can also be used (as is generally done) to compare to a given specification. However, the extension of laboratory to field lifetime prediction is much more subjective. Nevertheless, it was done on the basis of laboratory-to-field total radiations at incubation halflives. The results for Phoenix, Arizona, are offered accordingly. Overall, the major disadvantage in the entire process is the extremely long incubation times required to reach halflife for the more robust or specially formulated products. As noted on the various response curves, these times can reach 70 000 light hours at the lower incubation temperature of 60°C for the more robust geomembranes, which equates to approximately 10 years of laboratory incubation time plus the accompanying device maintenance, testing and analysis. The reader might appreciate that this paper represents the longest continuous research effort ever conducted by the Geosynthetic Institute.

ACKNOWLEDGEMENTS

This research project was sponsored by membership in the Geosynthetic Institute. As such, the authors sincerely appreciate the current (and past) members, affiliated members and associate members. The current list is available on the GSI website at www.geosynthetic-institute.org along with the current board of directors and other contact information. This paper is a modified version of a keynote paper delivered by the first author at the 3rd Pan-American Conference on Geosynthetics that was hosted by the North American Geosynthetics Society and held under the auspices of the International Geosynthetics Society (IGS) in April 2016 in Miami, Florida, USA. The authors and editor of the journal are grateful to the publisher of the conference proceedings (Minerva - Technology, Resources, and Information, Jupiter, Florida, USA) for permission to reproduce this paper.

NOTATION

Basic SI units are given in parentheses.

E_{act}/R	slope of semilog plot, i.e., activation energy (K)
OIT	oxidation induction time (s)
r	reaction rate (s)
R^2	statistical reliability (dimensionless)
T	temperature (deg K or deg C)
T-site	site-specific (lower) target temperature (deg K)
T-test	incubated (high) temperature (deg K)
UV	ultraviolet radiation (m)

REFERENCES

Allen, S. (2016). Geotextile durability. In *Geotextiles: From Design to Applications*, Koerner, R. M., Editor, Woodhead Publishing Co., Amsterdam, the Netherlands, pp. 177–216.

ASTM D746 Standard test method for brittleness temperature of plastics and elastomers by impact. ASTM International, West Conshohocken, PA, USA.

ASTM D1388 Standard test methods for the stiffness of fabrics. ASTM International, West Conshohocken, PA, USA.

ASTM D3895 Standard test method for oxidative-induction time of polyolefins by differential scanning calorimetry. ASTM International, West Conshohocken, PA, USA.

ASTM D4355 Standard test method for deterioration of geotextiles by exposure to light, moisture and heat in a xenon arc type apparatus. ASTM International, West Conshohocken, PA, USA.

ASTM D5885 Standard test method for oxidative-induction time of polyolefin geosynthetics by high pressure differential scanning calorimetry. ASTM International, West Conshohocken, PA, USA.

ASTM D7176 Standard specification for nonreinforced polyvinyl chloride (PVC) geomembranes used in buried applications. ASTM International, West Conshohocken, PA, USA.

ASTM D7238 Standard test method for effect of exposure of unreinforced polyolefin geomembranes using fluorescent UV condensation apparatus. ASTM International, West Conshohocken, PA, USA.

Barrett, B. (1966). Use of plastic filters in coastal structures. *Proc. 16th Intl. Conf. on Coastal Engineering*, Tokyo, Japan. Japanese Society of Soil Mechanics and Foundations, Tokyo, Japan, pp. 1048–1067.

Cazzuffi, D. (2014). Long-time behaviour of exposed geomembranes used for the upstream face rehabilitation of Dams in Northen Italy. *Proceedings of the 10th International Conference on Geosynthetics*, Berlin. German Geotechnical Society, Berlin, Germany, pp. 12 (CD-ROM).

Davis, G. W. (1989). Aging and durability of polyester geotextiles. In *Durability and Aging of Geosynthetics*, Koerner, R. M., Editor, Elsevier Publ., Co., Rotterdam, the Netherlands, pp. 65–81.

Elias, V., Christopher, B. R. & Berg, R. R. (2001). *Mechanically Stabilized Walls and Slopes Design*, Report No. FHWA-NHI-00-034. Federal Highway Association, Washington, DC, USA.

Giroud, J. P., Gourc, J.-P., Bally, P. and Delmas, P. (1977). Behavior of a nonwoven fabric in an earth dam. In *Intl. Conf. on the Use of Fabrics in Geotechnics*. Assoc. Amicole des Ingenieurs Anciena Eleves, Paris, France, pp. 213–218.

Greenwood, J. H., Schröder, H. F. & Voskamp, W. (2015). *Durability of Geosyntehtics*, 2nd edn. SBRCURnet/CRC Press, London, UK.

Haliburton, T. A., Fowler, J. & Langan, J. P. (1980). Design and construction of a fabric reinforced test section at Pinto Pass. *Mobil, Alabama, Trans. Res. Record #79*, National Highway Institute, Washington, DC, USA, pp. 49–58.

Hawkins, W. M. (2008). Geotextiles in unpaved roads: a 35-year case history. *Geosynthetics Magazine*, **26**, No. 3, 26–32.

Haxo, H. E. (1988). *Lining of Waste Containment and Other Impoundment Facilities*, EPA/600/2-82/02. U.S. EPA, Cincinnati, OH, USA.

Hsuan, Y. G., Schröder, H. F., Rowe, R. K., Müeller, W., Greenwood, J. H., Cazzuffi, D. & Koerner, R. M. (2008). Long-term performance and lifetime prediction of geosynthetics. *Proc. 4th European Conf.*, Edinburgh, Scotland, UK Chapter, International Geosynthetics Society, London, UK, pp. 512–521.

Ionescu, A., Kiss, S., Dragan-Balenda, M. *et al.* (1982). Methods used for testing the bio-colmatation and degradation of geotextiles. *Proc. 2nd ICG*. IFAI Publ., St. Paul, MN, USA, pp. 547–552.

Kane, J. D. & Widmayer, D. A. (1989). In *Durability and Aging of Geosynthetics*, Koerner, R. M., Editor, Elsevier Publ., Co., Rotterdam, the Netherlands, pp. 13–27.

Kırbaş, Z., Keshin, N. & Guner, A. (1999). Biodegradation of polyvinylchloride (PVC) by white rot fungi. *Bull. Environ. Contamin. Toxicol.*, **63**, No. 2, 335–342.

Koerner, R. M. (2012). *Designing with Geosynthetics*, 6th edn. Xlibris Publ. Co., Indianapolis, IN, USA.

Koerner, R. M. & Koerner, J. R. (2011). GMA Techline's Qs and As. *Geosynthetics Magazine*, **29**, No. 2, 40–44.

Koerner, R. M. & Koerner, G. R. (2014). Monitoring in-situ conditions at landfills for the purpose of evaluating long-term geomembrane performance. *Proc. 10th IGS*, German Geotechnical Society, Berlin, Germany.

Liang, D. W., Zhang, T., Fang, H. H. P. & He, J. (2008). Phthalates biodegradation in the environment. *Appl. Microbiol. Biotechnol.*, **80**, No. 2, 183–193.

Martin, J. R. & Gardner, R. J. (1983). Use of plastics in corrosion resistance instrumentation. *Paper Presented at 1983 Plastic Seminar, NACE*, Dallas, Texas, pp. 24–27, Society of Plastics Engineering, Washington, DC, USA, pp. 13–27.

Nalli, S., Cooper, D. G. & Nicell, J. A. (2011). Biodegradation of plasticizers by Rhodococcus rhodochrous. *Biodegradation*, **13**, No. 1, 343–352.

NREL (National Radiation Energy Laboratory) (2012). U. S. Dept. of Interior, Washington, DC, USA.

PGR (Polymer Grid Reinforcement) (1984). Thomas Telford Press, London, UK.

Rios, N. & Gealt, M. A. (1989). Biological growth in landfill leachate collection systems. In *Durability and Aging of Geosynthetics*, Koerner, R. M., Editor, Elsevier Publ., Co., Rotterdam, the Netherlands, pp. 244–259.

Scuero, A. M. & Vaschetti, G. L. (1996). Geomembranes for masonry and concrete dams: state of the art report. *Proceedings of the 1st European Geosynthetics Conference EuroGeo 1*, Balkema, Rotterdam, the Netherlands, pp. 889–896.

Staff, C. E. (1984). The foundation and growth of the geomembrane industry in the United States. *Proc. Intl. Conf. on Geomembranes*, Denver, Colorado. IFAI Publ., St. Paul, MN, USA, pp. 5–8.

3 Tier (2011). http://www.3tier.com/en/support (accessed 30/03/2011).

van Zanten, R. V. (1986). *Editor, Geotextiles and Geomembranes in Civil Engineering*, A. A. Balkema, Rotterdam, the Netherlands.

The Editor welcomes discussion on all papers published in Geosynthetics International. Please email your contribution to discussion@geosynthetics-international.com